Thin Solid Films 519 (2011) 2477–2482

Contents lists available at ScienceDirect

Thin Solid Films

journal homepage: www.elsevier.com/locate/tsf

Free transverse vibrations of cracked nanobeams with surface effects

By Seyyed M. Hasheminejad [a], Behnam Gheshlaghi [a,*], Yaser Mirzaei [b,*], Saeed Abbasion [c]

[a] Acoustics Research Laboratory, Department of Mechanical Engineering, Iran University of Science and Technology, Narmak, Tehran 16846-13114, Iran
[b] Islamic Azad University of Damavand, Iran
[c] Swiss Federal Laboratories for Materials Testing and Research, Wood-Department, Dübendorf, Switzerland

ARTICLE INFO

Article history:
Received 22 June 2010
Received in revised form 24 September 2010
Accepted 15 December 2010
Available online 23 December 2010

Keywords:
NW
Crack
Surface elasticity/tension
Euler–Bernoulli beam
Free vibration

ABSTRACT

The flexural vibrations of cracked micro- and nanobeams in the presence of surface effects are studied. The cracked-beam model is set up by dividing the classical cracked beam element into two segments connected by a rotational spring located at the cracked section. This model promotes a discontinuity in bending slope, which is proportional to the second derivative of the displacements. Numerical examples demonstrate the effects of beam length, and crack position and severity on the calculated values of natural frequencies of an anodic alumina nanowire in the presence of surface effects. Limiting cases are considered and good agreements with the data available in the literature are obtained.

1. Introduction

In classical continuum mechanics, the effect of surface energy is ignored as it is small compared to the bulk energy. For nanoscale materials and structures, however, the surface effects become significant due to the high surface/volume ratio. Both the atomistic simulations and experimental evaluations strongly suggested that the ratio of surface to volume plays a critical role in nanosized problems. To account for the effect of surfaces/interfaces on mechanical deformation, Gurtin et al. [1, 2] presented the surface elasticity theory by modeling the surface as a two dimensional membrane adhering to the underlying bulk material without slipping. Dingreville and Qu [3] introduced several interfacial elasticity tensors to fully characterize the elastic behavior of a bimaterial interface. Nozieres and Wolf [4] recognized the necessity of including the transverse deformation of the interface in computing the interfacial excess energy. The equilibrium and constitutive equations in the bulk of the solid are the same as those in the classical theory of elasticity, but the presence of surface stress gives rise to a nonclassical boundary condition. As the dimensions of a structure approach the nanoscale, the properties and elastic field can be size-dependent. For example, Wong et al. [5] by experimental study on the elastic bending of SiC nanobeams showed a change in the bending modulus while the diameter of the beam changes. The reason for such the size-dependency behavior at nanoscale is the presence of free surfaces, and the comparable fraction of energy stored in the surfaces with that in bulk for nanoscale structures. So, in order to fulfill nanoscaled promising applications, the size dependency of mechanical properties of such structures need to be sufficiently understood.

Mechanics of nanoscale objects are well stated concerning the effects of surface and interfacial energies. Gibbs [6] considered the effects of surface and interfacial energies and formulated the surface stress theory based on thermodynamics of solid surfaces. Murdoch [7] developed a general theoretical framework for a continuum with surface stresses and proposed a linearized surface stress–strain constitutive relation in which the surface domain is assumed to be very thin and has different elastic moduli from the bulk, and the surface adheres to the bulk without slipping. Several other researchers have contributed to further development of the surface stress theory [8–10], and some applied the surface stress theory to examine several issues involving nanoscale problems. For instance, Sharma et al. [11] analyzed the size-dependent elastic stresses of nanoinhomogeneities by surface elasticity theory. Dingreville et al. [12] illustrated the size effects on the elastic properties of nanosized particles, wires, and films induced by surface energy. Gao et al. [13] developed a finite element method to account for the effect of surface elasticity and analyzed the size-dependent mechanical behavior of several nanosystems. Also, Park and co-workers developed a finite element method based on the surface Cauchy–Born model to capture surface stress effects on nanomaterials within a continuum mechanics framework [14, 15]. There are also some works done about the importance of defects on the structures or intact devices behavior. For example Luque et al. [16] studied the surface cracks effect on the tensile behavior of cylindrical copper wires of nanometric diameter.

* Corresponding author. B. Gheshlaghi is to be contacted at Acoustics Research Laboratory, Department of Mechanical Engineering, Iran University of Science and Technology, Narmak, Tehran 16846-13114, Iran. Tel.: 98912 6189871, fax: 9821 77240488. Mirzaei, Islamic Azad University of Damavand, Iran. Tel.: 98912 2268159; fax: 9821 77240488.
E-mail addresses: behnamqeshlaqi@gmail.com (B. Gheshlaghi), mirzaei@damavandiau.ac.ir (Y. Mirzaei).

0040-6090/$ – see front matter © 2010 Elsevier B.V. All rights reserved.
doi:10.1016/j.tsf.2010.12.143

The crack in the structure of solids remains a fundamental issue both in theoretical research and in engineering applications. Cracks can appear in structural elements as a consequence of initial defects within the material or caused by fatigue during their operational life. They can reduce the structure's natural frequencies because it becomes more flexible. Many studies have adopted simplified procedures based on classical elasticity theory to evaluate the influence of the various parameters (e.g., crack length, crack location, boundary conditions, etc.) on the natural frequencies, saving the computing time of full finite element analysis. In particular, most researchers simply assumed the crack remains open throughout the period of vibration and have neglected the nonlinear influences of the Beam Length, L(m) breathing cracks for small vibration amplitudes [17–20]. The presence of the crack, and the corresponding reduction of the flexural beam stiffness, has been represented by means of linear massless rotational springs [21, 22], whose stiffness may be related to the crack properties by the fracture mechanics theory [23]. Fernandez-Saez and Navarro [17] presented an analytical method to calculate the fundamental frequency of cracked Euler–Bernoulli beams. The influence of the crack was represented by an elastic rotational spring connecting the two segments of the beam at the cracked section. Closed-form expressions for the approximated values of the fundamental frequency of cracked Euler–Bernoulli beams in bending vibration were given. More recently, Loya et al. [19] modified the classical cracked Euler–Bernoulli beam model to study the free flexural vibrations of cracked micro- and nanobeams, based on the nonlocal elasticity theory. The cracked nanobeam was modeled using a rotational spring located at the cracked section, which promotes a discontinuity proportional to the crack severity in the slope. In present study, following the classical approach first proposed by Freund and Hermann [21], and further followed by many others [17–20], we model the cracked beam as two beam segments connected by a rotational spring, to explore the surface effects on the free vibrations of cracked nanowires (NWs), based on the Euler–Bernoulli beam model.

2. Formulation

2.1. Free vibration of an intact nanowire

Taking in to account both surface elasticity and residual surface tension, flexural vibration of nanowires may be described by the simplified Euler–Bernoulli beam model, which is valid for long NWs, in the form [24]

$$(EI)^* \frac{\partial^4 v}{\partial x^4} + \rho A \frac{\partial^2 v}{\partial t^2} - p(x) = 0, \tag{1}$$

where $(EI)^* (= EI + E^s bh^2/2 + E^s h^3/6)$ is the effective bending modulus [24–26] with E being Young's modulus of the bulk, τ^0 being the surface stress along the NW longitudinal direction, E^s is the surface elastic modulus, $I = bh^3/12$ the cross section moment of inertia, b and h the width and the thickness of NW, respectively, ρ and A are density and cross section area, respectively, and $p(x) (= H\partial^2 v/\partial x^2)$ is the resulting distributed transverse force induced by surface effects along the NW longitudinal direction [3, 24, 27], also $H = 2\tau^0 b$ [24]. For free vibrations, the transverse displacement is assumed to be of the form $v(x,t) = V(x)e^{i\omega t}$, with ω being the radial frequency. Consequently, after introducing the dimensionless variables, $\xi = x/L$, $\lambda^4 = \rho A L^4 \omega^2/$

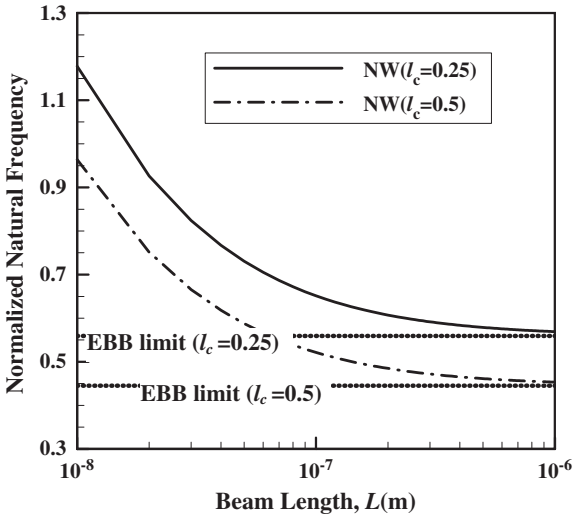

Fig. 2. Calculated normalized fundamental natural frequency as a function of beam length, for selected crack severity ($K = 2$) and crack positions.

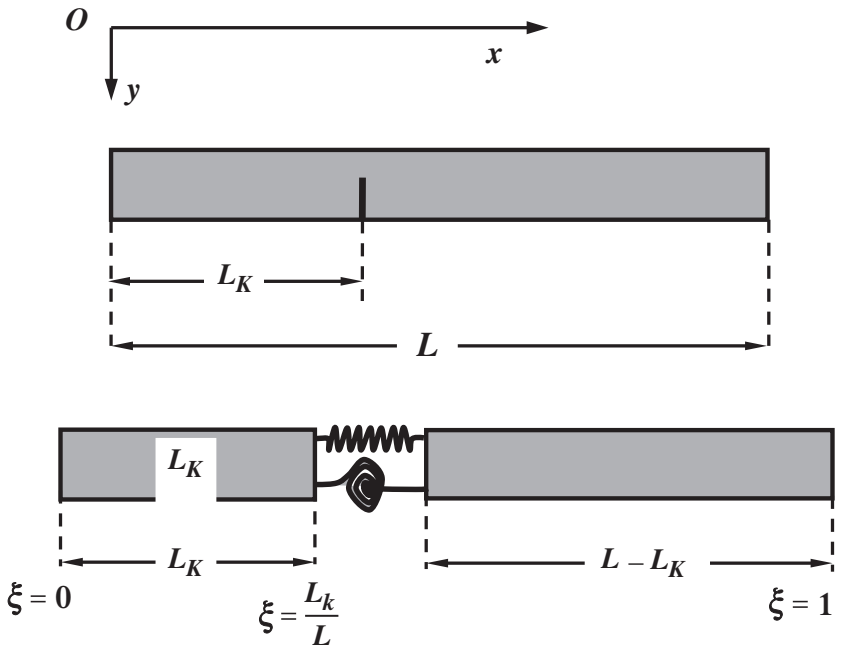

Fig. 1. Model of the cracked nanowire.

$(EI)^*$, $\bar{V} = V/L$, and $\eta = 2\tau^0 bL^2/(EI)^*$, the equation of motion (Eq. (1)) is simplified in the form

$$\bar{V}^{IV} - \eta\,\bar{V}'' - \lambda^4\,\bar{V} = 0, \tag{2}$$

where prime denotes differentiation with respect to the variable ξ. General solution for the above differential equation is written as

$$\bar{V}(\xi) = A_1\sinh(\Lambda_1\xi) + A_2\cosh(\Lambda_1\xi) + A_3\sin(\Lambda_2\xi) + A_4\cos(\Lambda_2\xi), \tag{3}$$

where $\Lambda_{1,2}^2 = \frac{\eta}{2} \pm \sqrt{\frac{\eta^2}{4} + \lambda^4}$.

2.2. Free vibration of a cracked nanowire

Consider a NW with an edge crack located at the distance L_K from the left end with the corresponding dimensionless variable $l_c = L_K/L$ (see Fig. 1). Also, let $\Delta\theta$ and Δu, respectively, be the rotated angle by the rotational spring and the relative horizontal displacement at $x = L_K$, described as [19]

$$\begin{aligned} \Delta\theta &= k_{MM}\frac{\partial^2 v}{\partial x^2} + k_{MN}\frac{\partial u}{\partial x}, \\ \Delta u &= k_{NN}\frac{\partial u}{\partial x} + k_{NM}\frac{\partial^2 v}{\partial x^2}, \end{aligned} \tag{4}$$

where k_{NN}, k_{MM}, k_{MN}, and k_{NM} are the flexibility constants. In the case of free flexural vibrations, no longitudinal displacement is considered ($u(x, t) = 0$), and the flexibility constants k_{NN}, k_{MN}, and k_{NM} are generally assumed to be small [19]. Thus, the slope increment may conveniently be written in the dimensionless form

$$\Delta\theta = \frac{k_{MM}}{L}\frac{\partial^2\bar{V}(\xi)}{\partial\xi^2}\bigg|_{\xi=l_c} = K\frac{\partial^2\bar{V}(\xi)}{\partial\xi^2}\bigg|_{\xi=l_c}, \tag{5}$$

where $K = \frac{k_{MM}}{L}$.

Now, keeping the equation of motion (Eq. (1)) in mind, the free vibrations of the two segments of the cracked NW are described by [19]

$$\begin{aligned} &\bar{V}_1^{IV} - \eta\,\bar{V}_1'' - \lambda^4\,\bar{V}_1 = 0, \quad 0 \le \xi \le l_c, \\ &\bar{V}_2^{IV} - \eta\,\bar{V}_2'' - \lambda^4\,\bar{V}_2 = 0, \quad l_c \le \xi \le 1, \end{aligned} \tag{6}$$

with the solutions

$$\begin{aligned} \bar{V}_1(\xi) &= A_1\sinh(\Lambda_1\xi) + A_2\cosh(\Lambda_1\xi) + A_3\sin(\Lambda_2\xi) \\ &\quad + A_4\cos(\Lambda_2\xi), \quad (0 \le \xi \le l_c), \\ \bar{V}_2(\xi) &= A_5\sinh(\Lambda_1\xi) \\ &\quad + A_6\cosh(\Lambda_1\xi) + A_7\sin(\Lambda_2\xi) + A_8\cos(\Lambda_2\xi), \quad (l_c \le \xi \le 1). \end{aligned} \tag{7}$$

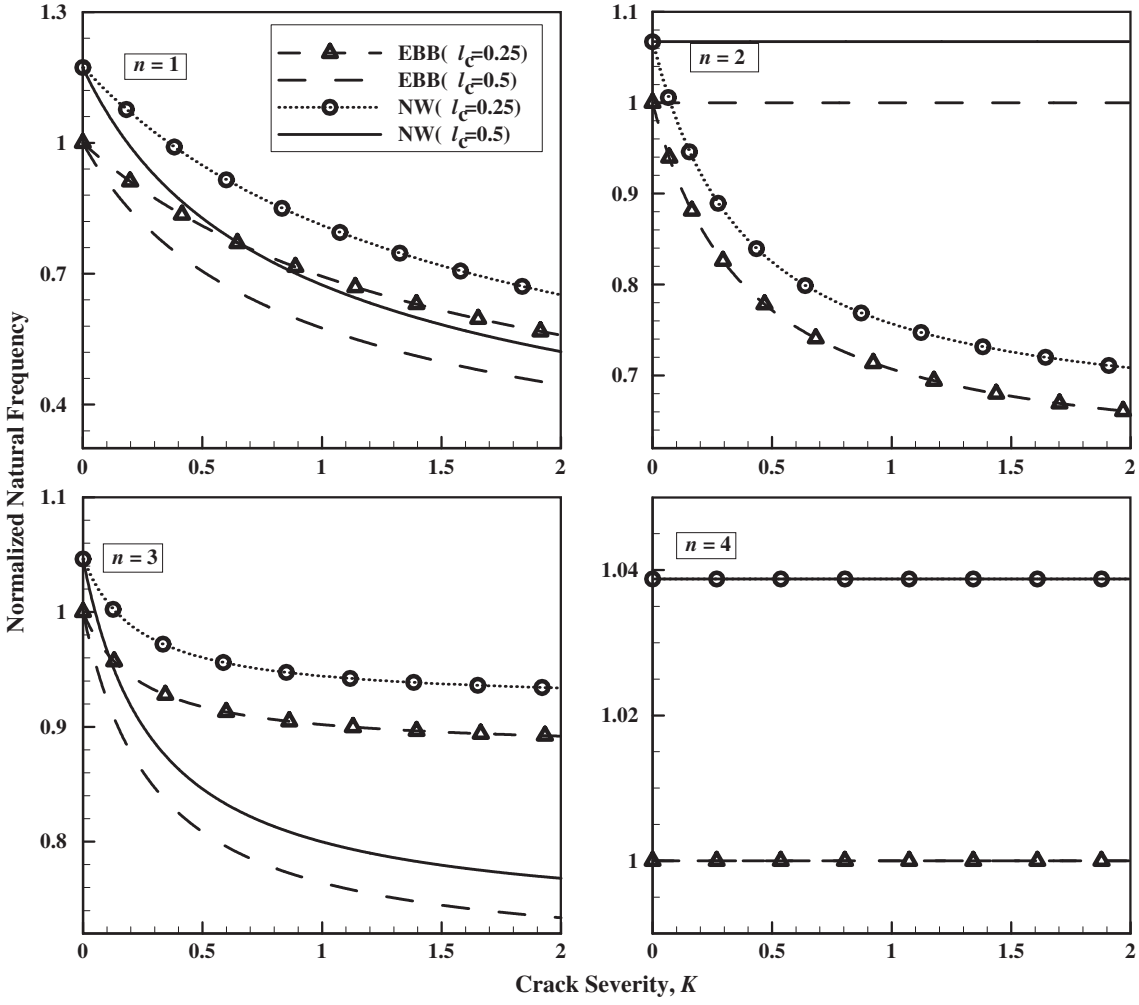

Fig. 3. First four computed normalized natural frequencies as a function of crack severity for selected crack positions and beam length ($L = 100$ nm).

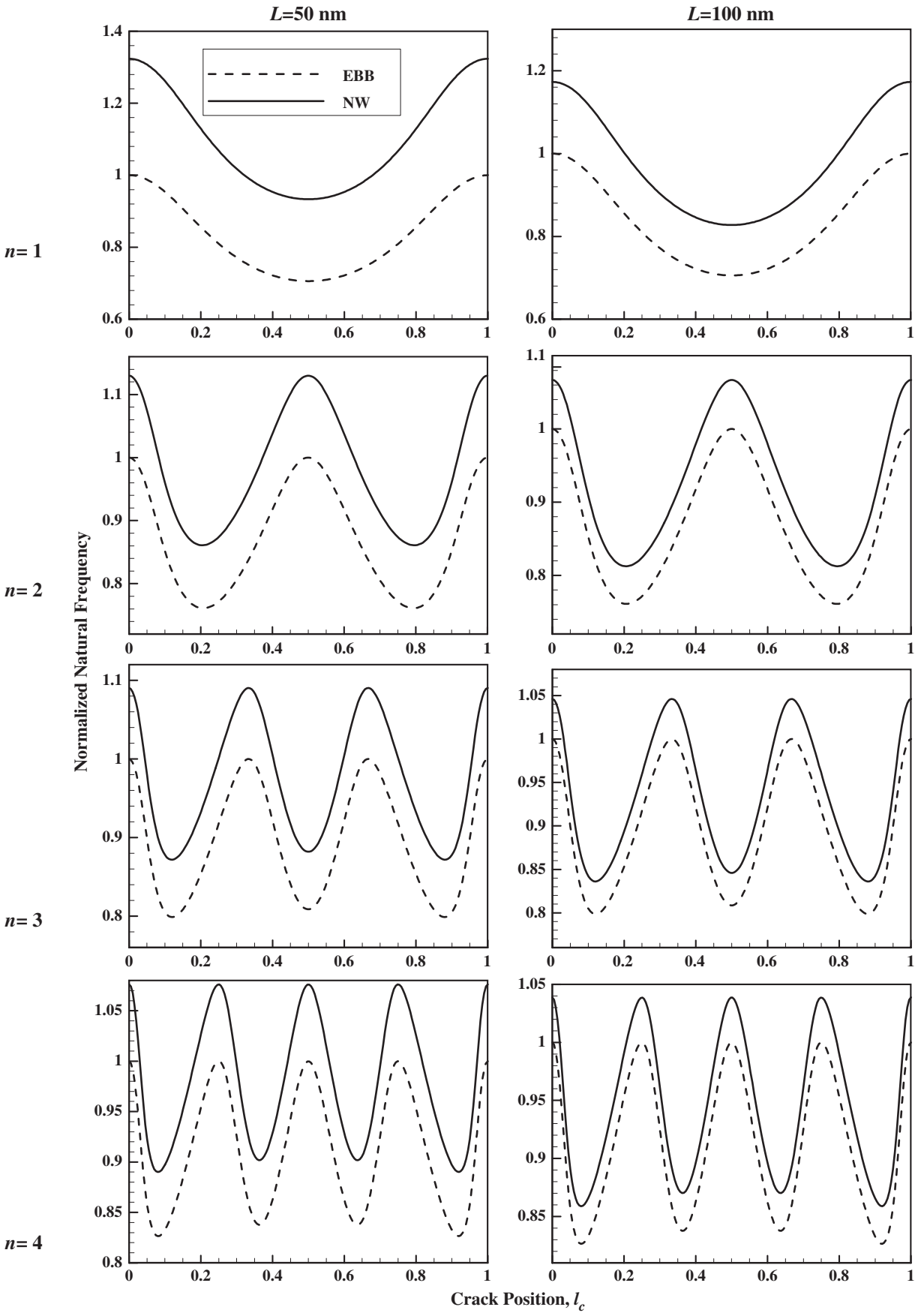

Fig. 4. First four calculated normalized natural frequencies as a function of crack position, for selected beam lengths and crack severity ($K = 0.5$).

The unknown coefficients A_1 through A_8 must be obtained by application of the classical simply-support boundary conditions [28] along with the relevant compatibility conditions [19], i.e.,

$$\begin{aligned} &\bar{V}_1(0) = \bar{V}_2(1) = 0,\ \bar{V}_1''(0) = \bar{V}_2''(1) = 0,\\ &\bar{V}_2(l_c) = \bar{V}_1(l_c), \Delta\theta = \bar{V}_2'(l_c) - \bar{V}_1'(l_c) = K\,\bar{V}_1''(l_c),\\ &\bar{V}_2''(l_c) = \bar{V}_1''(l_c),\ \bar{V}_2'''(l_c) = \bar{V}_1'''(l_c). \end{aligned} \tag{8}$$

Direct substitution of the solutions (Eq. (7)) into the above constraint equations yields a linear system of equation, whose determinant forms the system characteristic equation, ultimately leading to determination of the natural frequencies. This completes the necessary background required for the analysis of the problem. Next we consider some numerical examples.

3. Numerical examples

To illustrate the surface effects on the dynamic behaviour of cracked NWs, some numerical examples are presented in this section. A nanowire of selected thickness and cross section ($h=0.1L$, $A=h^2$) is considered to be made of anodic alumina with the [111] crystallographic direction and the physical properties: $E=70$ GPa, $y=0.3$, $\rho=2700$ kg/m^3; $E^s=5.1882$ N/m and $\tau^0=0.9108$ N/m [29] (here it is noteworthy that [100] and [111] surfaces are isotropic, while [110] surface is anisotropic). A Mathematica code [30] was constructed for numerical treatment of the (6×6) constraint equations (Eq. (8)), i.e., to calculate the system natural frequencies as a function of the beam length, crack position and severity through frequency sweeping in a simple root finding technique based on the bisection approach.

Fig. 2 shows the calculated normalized fundamental ($n=1$) natural frequency, $\Omega_n = n^2\pi^2\omega/\sqrt{\rho AL^4/EI}$, as a function of beam length (10 nm$\le L\le$1 μm), for selected crack positions ($l_c=0.25$, 0.5) and crack severity ($K=2$). Here, it is clear that for the material considered (i.e., anodic alumina with the [111] crystallographic direction), as the beam length increases (surface effects decreases), the natural frequencies (overall beam stiffness) gradually decrease, approaching the constant limits set by the Euler–Bernoulli beam theory. Also, the beam with the central crack ($l_c=0.5$) has a lower natural frequency than the (stiffer) beam with the non-central crack ($l_c=0.25$), which is as expected.

Fig. 3 displays the first four computed normalized natural frequencies, $\Omega_n = n^2\pi^2\omega/\sqrt{\rho AL^4/EI}(n=1,2,3,4)$ as a function of crack severity for selected beam length ($L=100$ nm), and crack positions $l_c=0.25$, 0.5. Also shown are the corresponding results based on the Euler–Bernoulli beam theory. The most important observations are as follows. While increasing the crack severity leads to a gradual decrease of the natural frequencies in the cases of $n=1$, 3 ($l_c=0.25$, 0.5); and $n=2$ ($l_c=0.25$), it does not have any impact in the cases of $n=2$ ($l_c=0.5$); and $n=4$ ($l_c=0.25$, 0.5). This may be explained by the fact that, for example, none of the crack positions $l_c=0.25$, 0.5 for the beam vibrating in first or third mode ($n=1$, 3) lie on the vibration nodes, while in the case of the $n=4$ mode, both crack positions ($l_c=0.25$, 0.5) are exactly set on the vibration nodes. Consequently, in the latter case ($n=4$) all natural frequency curves are entirely invariant with respect to the crack severity. Thus, one can conclude that in general the crack severity has no effect on the system natural frequencies when nl_c is an integer number.

Fig. 4 shows the first four calculated normalized natural frequencies, $\Omega_n = n^2\pi^2\omega/\sqrt{\rho AL^4/EI}(n=1-4)$, as a function of crack position, for selected beam lengths ($L=50$, 100 nm), and crack severity ($K=0.5$). Also shown are the corresponding results based on the Euler–Bernoulli beam theory. The most important observations are as follows. As noted earlier (see Fig. 2), the differences between the natural frequencies of Euler–Bernoulli beam and those of the nanowire decrease, as the beam length increases (surface effects decrease), especially for the higher mode numbers. This difference, which may be considered as a measure of the surface effects vanishes progressively, as the mode number increases [24]. Furthermore, the cyclic behavior of the frequency curves indicates that the crack location has maximum effect on the natural frequencies when it is exactly located on the vibration antinodes. In particular, the maximum effects for n-th mode are observed at $l_c=L(2i-1)/2n$ ($1\le i\le n$).

Lastly, in order to check overall validity of the work, we entirely neglected the surface effects and set $E^s=\tau^0=0$ in our Mathematica code to compute the first four normalized natural frequencies, $\Omega_n = n^2\pi^2\omega/\sqrt{\rho AL^4/EI}(n=1-4)$, as a function of crack severity for selected crack position ($l_c=0.5$). The outcome, as displayed in Fig. 5a shows good agreement with the results presented in Fig. 2 of Ref. [19] without the nonlocal effects. Subsequently, we totally omitted the crack severity parameter and set $K=0$ in our Mathematica code to compute the normalized natural frequencies, $\Omega_n = n^2\pi^2\omega/\sqrt{\rho AL^4/EI}(n=1-4)$, for an intact ("crack-less") NW, as a function of mode number ($1\le n\le5$), for selected dimensionless surface effect parameters defined by $\alpha_1=2E^sh^3/EI$ and $\alpha_2=2\tau^0hL^2/\pi^2(EI+2E^sh^3)$. The outcome, as shown in Fig. 5b exhibits good agreements with the results presented in Fig. 2 of Ref. [24].

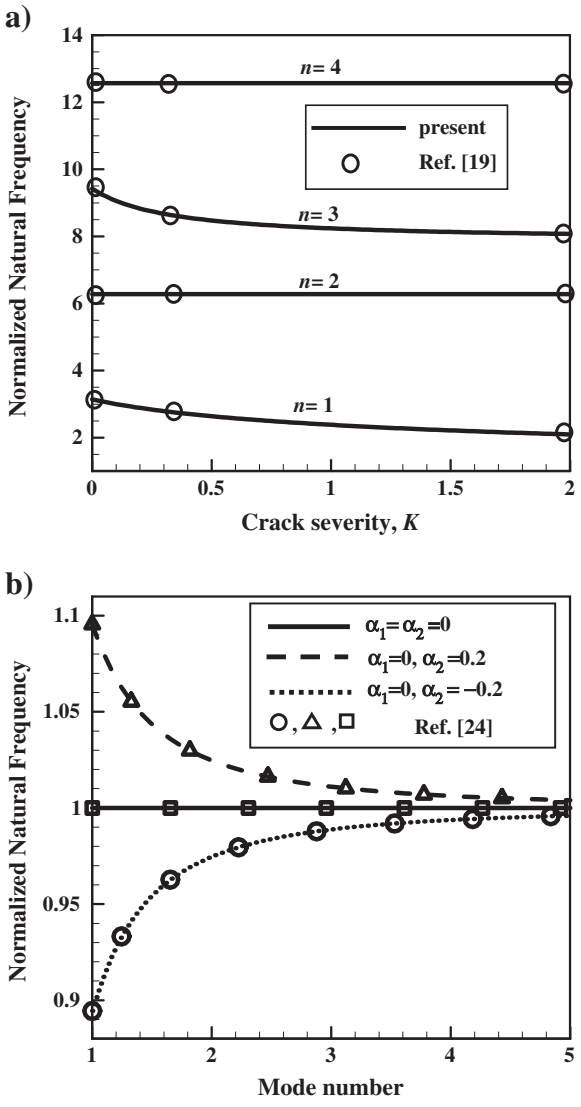

Fig. 5. Comparison of the computed natural frequencies in the limiting cases of (a) an Euler-Bernoulli beam with a central crack [19], (b) a nanowire without crack [24].

4. Conclusions

The free vibration of cracked nanowires considering the effects of surface elasticity and residual surface stress is studied. The Euler–Bernoulli beam theory is used, and the crack is modeled by a rotational spring representing the discontinuity in the slope and proportional to the crack severity. The key observations are summarized as follows. For the material considered, as the NW length increases (surface effects decreases), the natural frequencies (overall beam stiffness) gradually decrease, approaching the constant limits set by the Euler–Bernoulli beam theory. The beam with a central crack has a lower natural frequency than the relatively stiffer beam with a non-central crack. In particular, when the crack is precisely positioned at any vibration node, the natural frequencies become entirely insensitive with respect to the crack severity (e.g., when the product of mode number and the dimensionless crack position, nl_c is an integer number). Furthermore, the differences between the natural frequencies calculated based on the Euler–Bernoulli beam theory and those taking into account the surface effects decrease with increasing the beam size, especially as the mode number increases. Moreover, it is demonstrated that the crack location has a maximum effect on the natural frequencies when it is exactly located on the vibration antinodes (i.e., when $l_c = L(2i-1)/2n; 1 \le i \le n$). The proposed study may be of interest for the design, performance improvement, and health monitoring of nanowire-based components.

Acknowledgement

The authors wish to greatly thank the demanding reviewers whose constructive comments led to the significant improvement of the final manuscript.

References

[1] M.E. Gurtin, A.I. Murdoch, Arch. Ration. Mech. Anal. 57 (1975) 291.
[2] M.E. Gurtin, J. Weissmuller, F. Larche, Philos. Mag. A 78 (1998) 1093.
[3] R. Dingreville, J. Qu, J. Mech. Phys. Solids. 56 (2008) 1944.
[4] P. Nozieres, D.E. Wolf, Z. Phys. B. 70 (3) (1988) 399.
[5] E. Wong, P.E. Sheehan, C.M. Lieber, Science 277 (1997) 1971.
[6] J.W. Gibbs, The Scientific Papers of J. Willard Gibbs, Vol. 1, Thermodynamics Longmans and Green, New York, 1906.
[7] A.I. Murdoch, Q. J. Mech. Appl. Math. 29 (1976) 245.
[8] J.W. Cahn, F. Larche, Acta Metall. 30 (1982) 51.
[9] R.C. Cammarata, Prog. Surf. Sci. 46 (1994) 1.
[10] W.D. Nix, H. Gao, Scr. Mater. 39 (1998) 1653.
[11] P. Sharma, S. Ganti, N. Bhate, Appl. Phys. Lett. 82 (2003) 535.
[12] R. Dingreville, J.M. Qu, M. Cherkaoui, J. Mech. Phys. Solids 53 (2005) 1827.
[13] W. Gao, S.W. Yu, G.Y. Huang, Nanotechnology 17 (2006) 1118.
[14] H.S. Park, P.A. Klein, G.J. Wagner, Int. J. Numer. Methods Engrg. 68 (2006) 1072.
[15] H.S. Park, P.A. Klein, Phys. Rev. B 75 (2007) 085408.
[16] A. Luque, J. Aldazabal, J.M. Martinez-Esnaola, J. Gil Sevillano, Fatigue Fract. Eng. Mater. Struct. 29 (2006) 615.
[17] J. Fernandez-Saez, C. Navarro, J. Sound Vib. 256 (2002) 17.
[18] S. Zhong, S. Olutunde Oyadiji, J. Sound Vib 311 (2008) 328.
[19] J. Loya, J. Lopez-Puente, R. Zaera, J. Fernandez-Saeza, J. Appl. Phys. 105 (2009) 044309.
[20] L. Rubio, J. Fernandez-Saez, J. Vib. Acoust 132 (2010) 024504.
[21] L.B. Freund, G. Herrmann, J. Appl. Mech 76-APM-15 (1976) 112.
[22] R.D. Adams, P. Cawley, C.J. Pye, B.J. Stone, J. Mech. Eng. Sci. 20 (1978) 93.
[23] F.D. Ju, M. Akgun, T.L. Paez, E.T. Wong. Bureau of Eng. Res, Report No. CE-62(82) (1982) AFOSR-993-1.
[24] G.F. Wang, X.Q. Feng, Appl. Phys. Lett. 90 (2007) 231904.
[25] C.Q. Chen, Y. Shi, Y.S. Zhang, J. Zhu, Y.J. Yan, Phys. Rev. Lett. 96 (2006) 075505.
[26] J. He, C.M. Lilley, Nano Lett. 8 (2008) 1798.
[27] T. Chen, M.S. Chiu, C.N. Weng, J. Appl. Phys. 100 (2006) 074308.
[28] S. Rao, Vibration of Continuous Systems, Wiley, New Jersey, 2007.
[29] R.E. Miller, V.B. Shenoy, Nanotechnology. 11 (2000) 139.
[30] S. Wolfram, Mathematica: A System for Doing Mathematics by Computer, 2Addison Wesley Publishing Company, Reading, MA, 1991.